

The effect of curcumin in combination with radiation therapy and hyperthermia for a glioblastoma spheroid model

B. Ghanbari¹, A. Neshasteh Riz^{1,2}, Z. Hormozi Moghaddam^{1*}

¹Radiation Biology Research Center, Iran University of Medical Sciences, Tehran, Iran

²Department of Radiation Sciences, Allied Medicine Faculty, Iran University of Medical Sciences, Tehran, Iran

ABSTRACT

► Original article

*Corresponding authors:

Ali Neshasteh Riz, Ph.D.,

Z. Hormozi Moghaddam, Ph.D.,

E-mail:

neshastehriz@yahoo.com

hormozimoghaddam.z@iums.ac.ir

Received: February 2023

Final revised: June 2023

Accepted: July 2023

Int. J. Radiat. Res., January 2024;
22(1): 145-153

DOI: 10.52547/ijrr.21.21

Keywords: Glioblastoma multiforme, spheroid cell culture, curcumin, radiation, hyperthermia.

Background: The most common form of human primary brain tumor resistant to treatment is glioblastoma multiforme. For brain tumors, it is essential to optimize the treatment regimen with curcumin as a sensitizing agent and adjunctive to traditional or alternative therapy. This study aimed to determine the combined effects of cell death and apoptosis caused by curcumin before and after radiation with hyperthermia on glioblastoma in a monolayer cell culture and spheroid cell model. **Materials and Methods:** The spheroid cells were separately or simultaneously treated with the IC50% concentration of curcumin before and after 2 Gy radiation. Hyperthermia was then applied by incubating the cells at 43 °C for 1 hr. The survival rate of the cells was measured via the 3-(4,5-dimethylthiazol-2-yl)-2,5-diphenyl tetrazolium bromide (MTT) assay. Bax, Bcl-2, and caspase-3 expressions were quantified with real-time PCR (RT-PCR). **Results:** Cell viability significantly decreased in the curcumin (before) with radiation group (CCM+IR) by 51.12%, and in the radiation, curcumin, and hyperthermia group (IR+ CCM+ H) by 31.01%. The expression level of Bax and caspase-3 significantly increased in the combination of radiation, curcumin, and hyperthermia group (IR+ CCM+ H) by 3.80 ± 0.02 and 5.13 ± 0.12 , respectively. The Bcl-2 expression level in the radiation with curcumin and hyperthermia group was 0.41 ± 0.01 , compared to the curcumin before radiation group (0.70 ± 0.05) and the curcumin after radiation group (0.60 ± 0.02). **Conclusion:** Curcumin was more effective on cell death after radiation. It caused a synergistic effect in combination with other adjuvant therapies for glioblastoma spheroid cells.

INTRODUCTION

Recent studies indicate that glioblastoma is the brain's most common and aggressive cancer. Surgery is the first-choice treatment, followed by radiation therapy and chemotherapy. The survival rate of patients with glioblastoma multiforme (GBM) is short after diagnosis (1, 2). Glioblastoma is resistant to common cancer treatments. Some strategies such as using radio-sensitizers, optimizing treatment regimens, and combination therapy have been recommended to improve the response to treatment (3-5). This adjunctive therapy is often used after first-line treatments such as surgical and radiation therapy that reduce the chance of cancer recurrence. However, few primary and adjuvant therapies such as curcumin (CCM) have been studied for brain tumors (3, 5, 6).

Evidence indicates that apoptosis is a homeostasis process to keep cell populations under control in some cancers, including glioblastoma (7). Inhibition of apoptosis correlates with carcinogenesis and leads to drug resistance in glioblastoma (8-11). Many survival signaling mechanisms may be important in apoptosis inhibition, including overexpression of an apoptosis

inhibitor protein, factor kappa B (NF-κB), and anti-apoptotic Bcl-2 proteins (12-16). New therapeutic strategies, which can suppress the anti-apoptotic factors synergistically or increase pro-apoptotic factors in tumor cells to upregulate apoptosis, have been suggested to cure or prolong patients' life spans. Recently, studies indicated that radio-sensitization arrested the cancer cell cycle and enhanced apoptotic cellular pathways such as NFκB-, PI3-kinase- or p53-activity, and deoxyribonucleic acid (DNA)-double-strand breaks (5, 16).

CCM is a compound of diferuloylmethane obtained from turmeric (*Curcuma longa*). CCM has cancer treatment properties within in vitro and in-vivo models (17). CCM activates pathways depending on caspase to induce cell death and apoptosis in cancerous cells. In cells such as Caki cells, dephosphorylation of Akt suppresses Bcl-2, Bcl-xL, and IAPs, and increases the release of mitochondrial cytochrome c into the cytosol so that, following caspase-9, and caspase-3, it leads to cell death and apoptosis (16). Moreover, CCM induces apoptosis in human glioblastoma T98G cells (18) and leukemia HL-60 cells (19) by BID cleavage through caspase-8 and caspase-3 activation.

Furthermore, CCM actuates caspase-3-independent apoptosis in various cell types ⁽²⁰⁾. One of the most important factors of apoptosis is caspase-3, which can cause irreversible apoptosis ⁽²¹⁾. The major proteins in apoptosis and anti-apoptosis are Bax and Bcl-2. The expression ratio of these proteins can estimate the event of apoptosis. New research suggests that CCM prevents proliferation and invasion through the apoptosis pathway ^(22, 23). CCM might be effective against highly malignant glioblastoma U87MG cells. Further molecular investigations have been important in treating CCM as an effective anticancer drug. Adjuvant therapies, especially radiation therapy and hyperthermia, are unknown in terms of the expression of factors in GBM in different treatment regimens.

Using adjuvant treatment methods with CCM in GBM is a critical issue in radiation-induced apoptosis in treatment methods ⁽²⁴⁾. Therapeutic hyperthermia increases tissue temperature, usually in the range of 41 to 45 °C ⁽²⁵⁾. Hybridizing hyperthermia with radiation and chemotherapy has been successfully used in the treatment of cancerous cells. Although hyperthermia alone is not effective in cancer cell death, it is commonly used clinically as an adjunctive therapy along with radiation/chemotherapy for malignant diseases ^(26, 27). Fortunately, clinical trials have demonstrated the effectiveness of combined hyperthermia therapy to control tumor growth and increase survival in patients with various types of high-risk tumors. The major mechanism of mild hyperthermia is heat-induced cell apoptosis. Studies report that mitochondria, intrinsic, and death receptor pathways contribute to hyperthermia-induced cellular apoptosis ⁽²⁶⁻²⁸⁾. Furthermore, the effect of hyperthermia as an inhibitory method can be investigated to prevent cell repair and enhance glioblastoma treatment.

Based on the literature, CCM produces the most effective response to treatment after DNA damage ⁽²⁸⁾. Thus, this study aimed to examine the effect of CCM before and after radiation therapy with the hyperthermia method to approach the therapeutic goals and optimize the effective treatment regimen on glioblastoma cells under spheroid culture conditions. Considering their cell attachment and three-dimensional shape, the culture of spherical cells is mimicked in in vivo models ^(29, 30). Finally, this study provides empirical evidence of the combined effects of CCM-induced cell death and apoptosis before and after irradiation with hyperthermia on glioblastoma in monolayer and spheroid cell models to well recognize the function of CCM.

MATERIAL AND METHODS

Cell culture

The human glioblastoma cell line U87MG was cultured in Dulbecco's modified eagle medium

(DMEM) (Biowest Co., Nuaille, France) dissolved in 1% Pen-Strep (500 U/ml penicillin and 200 mg/l streptomycins (Biowest Co., Nuaille, France) and 10% fetal bovine serum (FBS) (Biowest Co., Nuaille, France).

Monolayer culture

The cells were cultured in a monolayer culture with a density of 2.5×10^5 cells/ml in T-25 cell culture flasks. The cell culture plate was incubated at 37 °C in 95% humidity and 5% CO₂. To check the logarithmic phase of the growth curve, the cells were grown until reaching a density of 70-80%. Detachment of cells was performed using 1 mM ethylenediaminetetraacetic acid (EDTA) and 0.25% (w/v) trypsin (Biowest, Nuaille, France) in phosphate-buffered saline (PBS) (DNAbiotech, Tehran, Iran). After each passage, cell viability <98% was confirmed using trypan blue.

Spheroid culture

Carlsson and Yuhas's description of the technique for overlaying liquids was used to form the spheroids ⁽³⁰⁾. The cells were placed in a T25 cell culture flask containing layer upon layer of poly (2-hydroxyethyl methacrylate) (poly HEMA) crystals and 10 ml of DMEM 10% FBS. The flask was kept at 37 °C in 95% humidity and 5% CO₂. The medium was changed twice a week.

According to equation 1, in the plot of the growth of the spheroid cell curve, the large and small diameters of almost 20 spheroids were randomly evaluated by a microscope every two days for a month.

$$V = a \times b^2 \times \frac{\pi}{6} \quad (1)$$

Where; the parameter "a" is the small axis/diameter and "b" is the large axis/diameter (μm) of the spheroid volume. In equation 2, the curve is shown according to the semi-logarithmic scale versus time. The volume of the spheroid in linear or logarithmic-phase curves equation 2:

$$V = V_0 \times e^{kt} \quad (2)$$

Where; V is a spheroid volume after time (t), V₀ is the primary volume, and k is the slope of the linear plot. The volume doubling time (VDT) is calculated from equation 3. The doubling time of the spherical volume was also estimated to determine the appropriate drug treatment time (equation 3).

$$VDT = \frac{\ln 2}{k} \quad (3)$$

Where; ln2 is 0.693 and k represents the line slope in the logarithmic phase in equation 2 and 3.

Converting spheroids to single cells

Spheroids were to be converted into a single cell for the experimental assay. Hence, the control and

treated groups were inserted into falcon tubes and centrifuged at 1200 rpm for 5 min. The cell culture medium was removed and the cell groups were centrifuged in 1 ml PBS again. The buffer was removed, and a 300-ml solution of trypsin/ EDTA (Biowest Co., Nuaille, France) was added to the tubes for 5 min. Cell-cell connections of spheroids affected by trypsin EDTA and the mechanical method were broken through resuspension of spheroids by micropipette into single cells. Finally, 700 ml of the medium containing 10% FBS was added to neutralize trypsin. Then, the cells were counted using a hemocytometer slide, and viability was determined.

Drug treatment (CCM)

CCM (Sigma Aldrich, USA) was dissolved in DMSO (Merck KGaA, Darmstadt, Germany); less than 0.20% was weekly kept at -80 °C for long-term storage and use at -20 °C.

Drug toxicity

The safety of CCM treatment on GBM cancer cells was examined by the MTT assay. To treat GBM cells, various CCM concentrations were used for 59 h. The GBM cancer cells were treated with different concentrations of CCM for 59 hr. Cell viability was calculated in comparison with the control group. The control contained the highest concentration of dimethyl sulfoxide (DMSO) dissolved in the drug. Half-maximal inhibitory concentration (IC₅₀) was calculated by linear regression in Excel (Microsoft Office 2019). All the experiments were performed in triplicate.

Combined treatment

The treatment protocol started when U87MG spheroids reached the desired diameter of 100 µm after almost a week. Incubation with IC₅₀ concentrations of CCM for 24 h was carried out to investigate the simultaneous effects of these treatments in the studied cell. Radiation was performed before or after adding CCM. Then, the cell groups were washed twice with PBS, and CCM was removed from the cell culture medium. The cells were inserted into the falcons and sealed. During hyperthermia, the cell suspension was kept in the culture medium without FBS and CCM. Practically, the spheroid cells were treated by a single modality like control (Con), radiation (IR), curcumin (CCM: 24-hour curcumin and 59-hour evaluation), and hyperthermia (H). The combination treatment included CCM (after) with radiation (IR+ CCM), CCM (before) with radiation (CCM+IR), radiation with hyperthermia (IR+H), curcumin with hyperthermia (CCM+H), and CCM (after) with radiation and hyperthermia (after) (IR+ CCM+H). For radiation, 2Gy dose X-ray was administered by a linear accelerator (LINAC) (Electa compact, Stockholm, Sweden) 6 MV photon beam, in a 20×20 field, with 97-cm source to

skin distance (SSD), 198 monitor units (MU).

Flasks (containing spheroids with a diameter of 100 µm) were sandwiched by 3-cm perspex on and 3-cm perspex under them. The radiation dose was distributed in the center of the perspex layers via a port. To obtain the ultimate concentrations of 25 µM and T-25 flasks containing spheroids with a diameter of up to 100 ml, 6.25 µl of CCM was administered per 4993.75 mL of the medium. All the groups that had to receive hyperthermia were incubated at 43 °C in a water bath (Mettmert Co., Schwabach, Germany) for 1 h. The hyperthermia time was monitored by a multi-logger thermometer (CHY FIREMATE Co. Model: CHY/502, Taiwan) in a water bath with a constant temperature of 43 °C. The treated groups were assessed 59 h after incubation. Then, spheroids were transferred to falcons washed twice with PBS, and centrifuged. Next, the spheroids were converted to single cells using a mechanical method and trypsin enzyme. All the cells in the falcons were returned to plates for the MTT assay and real-time polymerase chain reaction (real-time PCR: RT-PCR).

Cell viability assay

Treatment of glioblastoma U87 cells was evaluated by the MTT (3-[4,5-dimethylthiazol-2-yl]-2,5 diphenyl tetrazolium bromide) assay kit (DNAbiotech Co., Tehran, Iran). After the treatment protocol, 10000 cells of the groups were seeded in 96-well plates. The cells adhered during 24 h. To perform this assay, the medium was removed, and 100 µl of FBS-free medium and 10 µl of MTT (5 mg/ml in PBS) were added to each well and incubated for 4 h. Then, the medium was changed by 200 µl of DMSO. Optical density was measured by absorbance at 545 nm using an enzyme-linked immunosorbent assay (ELISA) reader (DANA Co., Model-DA3200, Iran). The relative survival rate was calculated as the absorption fraction of the treated sample/absorption of the control group. Measurements were performed for all the groups three times.

RNA isolation and RT-PCR

The isolation total ribonucleic acid (RNA) of the groups was extracted 24 h after the treatments by a total RNA extraction kit (Jena Bioscience Co., Jena, Germany) based on the manufacturer's instructions. Total RNA was collected from approximately 4×10^6 cells. A spectrophotometer was used to analyze optical density (OD). cDNA (complementary DNA) was synthesized according to the instructions (AccuPower CycleScript RT PreMix, Bioneer Inc., Korea). Clone Manager Professional 7 (Sci-Ed Software) and the National Center for Biotechnology Information (NCBI) site were used to design all the primer sequences. GAPDH was selected as an internal control. Table 1 lists the designated primer sequences. In the thermal gradient PCR, annealing temperatures were optimized for all the primers. The

RT-PCR SYBR Green (AccuPower GreenStar qPCR Master Mix, Bioneer Inc, Korea) technology was employed in all RT-PCR experiments conducted by Rotor Gene (Corbett Rotor- gene 6000, Sydney, Australia). For a total volume of 20 L, the reaction utilized 2 µl of the cDNA product, 10 µl SYBR green, 6 µl H₂O, and 2 µl of the forward and reverse primer. The RT-PCR program included pre-denaturation at 95 °C for 10 min. Denaturation was performed for 15 s at 95 °C and annealing at 61 °C, 60 °C, and 59 °C for 45 s. Extension was done at 72 °C for 1 min. Each sample was replicated three times (n = 3), and the mean was calculated. Cycle thresholds (CT) provided by RT-PCR were used to calculate the relative fold expression using the normalization of internal control GAPDH and untreated control group.

Table 1. Primer sequences for RT-PCR.

| Gene | Accession number | Forward oligo sequence | Reverse oligo sequence | Length gene (bp) |
|-----------|------------------|-----------------------------|-------------------------------|------------------|
| Bax | NM-001291428 | GGACGAACTGG ACAGTAACATGG | GCAAAGTAGAAA AGGGCGACAAC | 129 |
| Bcl-2 | NM-000633 | ATCGCCCTGTG GATGACTGAG | CAGCCAGGAGAA ATCAAACAGAG G | 150 |
| Caspase-3 | NM-032991 | ATGGAAGCGAA TCAATGGACTC | CTGTACCAGAC CGAGATGTCA | 138 |
| GAPDH | NM-001289745 | GAGTCAACGG ATTGGTCGT | GACAAGCTTC CCGTTCTCAG | 185 |

Statistical analysis

Three independent trials were used to present the data. Between-group comparisons were performed using t-tests, one-way analysis of variance (ANOVA), and Tukey's post hoc test. The significance level was $P \leq 0.05$ between the groups. Treatment protocol results were expressed as mean \pm standard deviation (SD). The data were analyzed by SPSS 26 (SPSS/PC Inc., Chicago, IL).

RESULTS

The growth rate of GBM spheroids

To further investigate the novel effects of curcumin on GBM cells, this examination was performed morphologically after spheroid formation (figure 1). The spheroid diameter reached 100 µm 8 to 10 days after seeding. The growth curve was plotted to determine the doubling time for drug treatment (figure 2). According to the logarithmic curve's gradient, VDT was calculated at approximately 58.77 h.

CCM affects GBM viability

Treatment of cells with increasing concentrations of CCM for 59 h decreased cell viability. Figure 3 shows the percentage of cell viability after treatment with different doses of CCM for 24 h. Drug toxicity for 5, 10, 15, 20, and 30 µM CCM was 93.59%, 75.65%, 68.08%, 60.76%, and 41.11% respectively. The control contained the highest concentration of DMSO. The concentration at 25 µM showed a 50.74%

viability and was considered IC₅₀. Thus, a CCM dose of 25 µM was selected for the following studies. According to linear regression, the IC₅₀ was 25.09 µM.

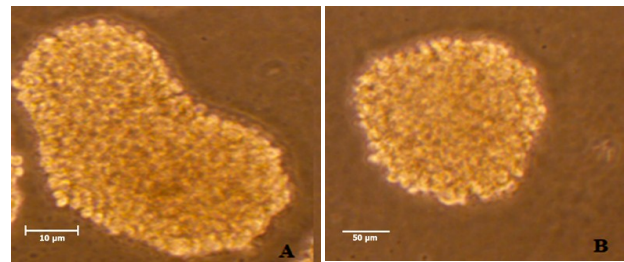


Figure 1. The microscope micrographs of the U87MG spheroids. **A)** 100-µm spheroid on day 9 (10 µm) ; **B)** 300-µm spheroid on day 20 (50 µm).

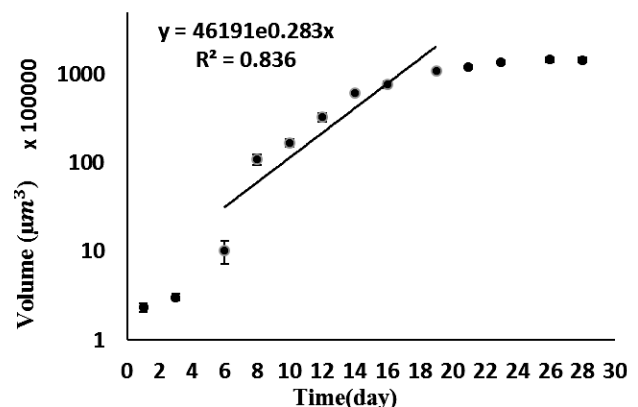


Figure 2. The growth curve of glioblastoma spheroid cells.

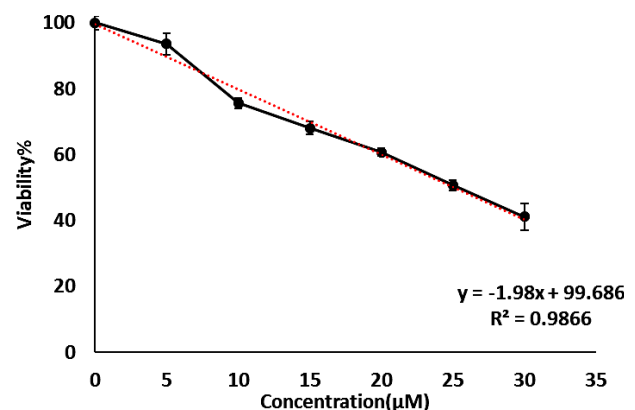


Figure 3. MTT assay to determine drug (CCM) concentration and control (DMSO) toxicity after 59 hours (n = 3).

After 59 h, the effect of selective concentration of CCM in combination with adjuvant therapies on GBM spheroids with a diameter of 100 µm evidently decreased the viability (figure 4). Significant differences in the viability of GBM spheroid were observed between the treatment, control, and radiation groups ($p < 0.01$). The minimum viability percent was significant in the combination group (IR+CCM+H) at 31.01% compared with other groups ($P < 0.0001$) (figure 4).

Cell death was between 15% and 36% when the treatment methods were used alone. The highest mortality belonged to the combination of

hyperthermia and CCM (CCM+H), with a viability of 40.52%. The survival rate of the radiation and hyperthermia (IR+H) group was 41.5%. Finally, the combination of CCM (before) with radiation (CCM+IR) group showed a rate of 60.88%, and the CCM (after) with radiation (IR+CCM) group had a rate of 51.12%. The effects of CCM in combination with other adjuvant therapies (IR+CCM+H) for GBM spheroid cells are depicted in figure 4.

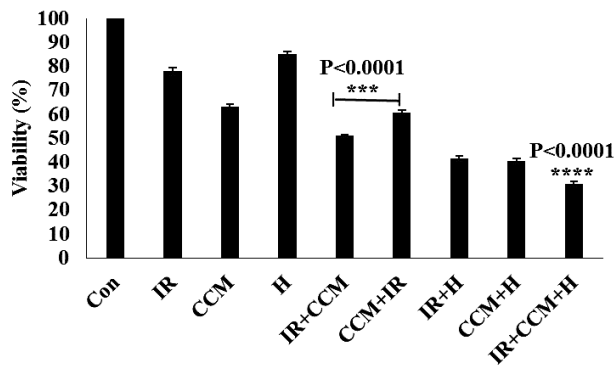


Figure 4. MTT assay results after doubling time (59 hours) treatments for different groups (Con: control, IR: 2Gy radiation, CCM: 25 μ M curcumin, H: hyperthermia (43 °C), IR+CCM: curcumin (after) with radiation, CCM+IR: curcumin (before) with radiation, IR+H: radiation and hyperthermia, CCM+H: curcumin with hyperthermia, IR+CCM+H: curcumin (after) with radiation and hyperthermia.) (n = 3). In each group bar standard division: * p < 0.05, ** p < 0.01, *** p < 0.001, **** p < 0.0001 (t-test and one-way ANOVA).

CCM, in combination with other adjuvant therapies, induced GBM spheroid apoptosis by increasing the Bax / Bcl-2 expression

Figures 5 a and b show the relative mean expression level of Bax and Bcl-2 genes, as well as the Bax-Bcl-2 ratio, in GBM spheroids after 24 hours of combined treatment. Based on the RT-PCR results, the expression of Bax mRNA (messenger RNA) in the combination group (IR+ CCM+ H) (3.80 ± 0.02) compared with the control group (1.00 ± 0.00) and single methods such as radiation (IR) (1.74 ± 0.03) and hyperthermia (H) (1.21 ± 0.01) (p<0.05) were significant. The expression level of Bax mRNA was significantly higher than in CCM (after) with radiation (IR+ CCM) (2.42 ± 0.02) group compared with CCM (before) with radiation (CCM+IR) (2.12 ± 0.02) (figure 5a).

The expression level of Bcl-2 mRNA in the group treated with radiation and hyperthermia in combination with CCM is displayed in figure 5a. The expression level of Bcl-2 mRNA significantly decreased in the radiation and CCM with hyperthermia (IR+CCM+H) group (0.41 ± 0.01) compared with the control group (1.00 ± 0.00). In addition, the expression level of Bcl-2 mRNA was significantly lower in CCM (after) with radiation (IR+ CCM) (0.60 ± 0.02) compared to CCM (before) with radiation (CCM+IR) (0.70 ± 0.02).

The Bax/Bcl2 ratio (figure 5b) denotes the

susceptibility of cells to the expression of genes related to apoptosis. The group treated with radiation in combination with CCM and hyperthermia showed a maximum Bax/Bcl-2 ratio. The expression level of Bax/Bcl-2 in this combination therapy changed the gene expression level in GBM spheroid cells.

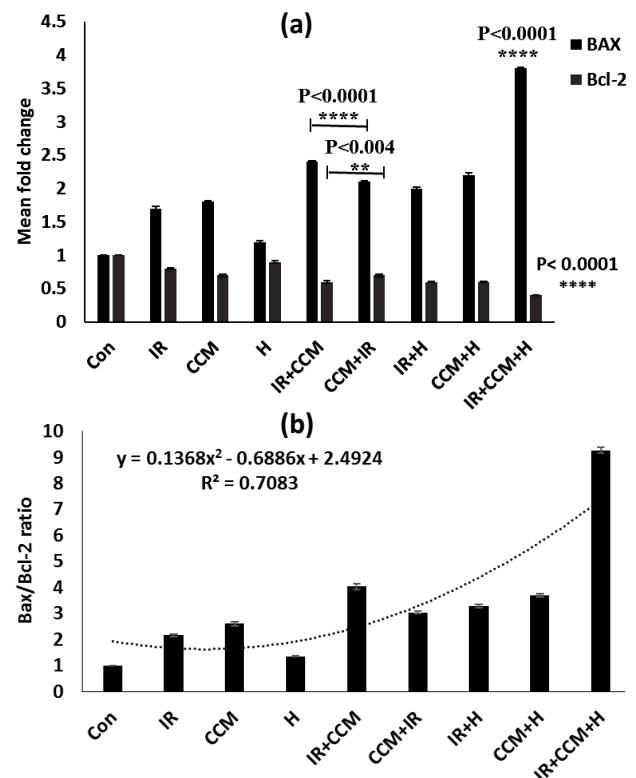


Figure 5. Relative fold change, a) Bax and Bcl-2 gene expression, b) Bax-Bcl2 ratio after treatments for different groups (Con: control, IR: 2Gy radiation, CCM: 25 μ M curcumin, H: hyperthermia (43 °C), IR+CCM: curcumin (after) with radiation, CCM+IR: curcumin (before) with radiation, IR+H: radiation and hyperthermia, CCM+H: curcumin with hyperthermia, IR+CCM+H: curcumin (after) with radiation and hyperthermia) (n = 3). In each group bar standard division: * p < 0.05, ** p < 0.01, *** p < 0.001, **** p < 0.0001 (t-test and one-way ANOVA).

CCM, in combination with other adjuvant therapies, induced apoptosis of GBM spheroid by increasing caspase-3 expression

Figure 6 illustrates the expression level of caspase-3 at 24 h following treatments and medium transfer. The RT-PCR results showed that the expression level of caspase-3 in the treated groups was significantly higher than in the control (1.00 ± 0.00) (p<0.05). The relative expression of caspase-3 differed in the treated groups with radiation and hyperthermia (IR+H) (2.81 ± 0.01) with radiation (IR) (2.20 ± 0.02) and hyperthermia (H) (1.20 ± 0.16) alone.

The mean change in caspase-3 expression was higher in CCM with hyperthermia (CCM+H) (2.90 ± 0.02) compared with CCM (1.81 ± 0.01) groups alone. The treated group with CCM (after) with radiation (IR+ CCM) (3.30 ± 0.02) had a more relative

expression of caspase-3 compared to the group treated with CCM (before) with radiation (2.91 ± 0.02) group.

The group treated with CCM in combination with adjuvant methods (5.13 ± 0.12) demonstrated the highest elevation of Caspase-3 expression. The expression level of caspase-3 also significantly affected gene expression (figure 6).

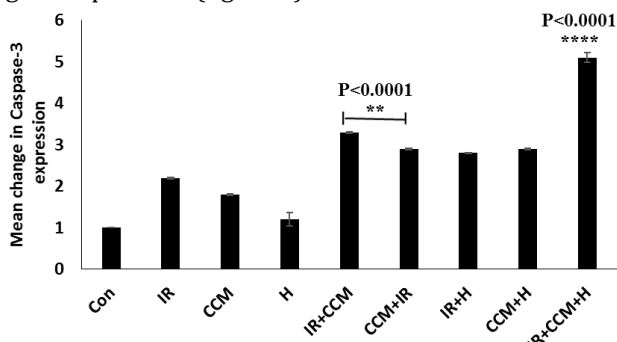


Figure 6. Relative fold change in caspase-3 gene expression 24 hours after treatment for different groups (Con: control, IR: 2Gy radiation, CCM: 25 μ M curcumin, H: hyperthermia (43 $^{\circ}$ C), IR+CCM: curcumin (after) with radiation, CCM+IR: curcumin (before) with radiation, IR+H: radiation and hyperthermia, CCM+H: curcumin with hyperthermia, IR+CCM+H: curcumin (after) with radiation and hyperthermia (n = 3). In each group bar standard division: * p < 0.05, ** p < 0.01, *** p < 0.001, **** p < 0.0001 (t-test and one-way ANOVA).

DISCUSSION

Due to the antitumor effects of CCM, it has been extensively studied (31-33) but its mechanisms are still unknown. Therefore, in the present study, it was hypothesized that CCM is more effective in cancer treatment after damaging DNA by radiation and can sensitize GBM spheroid cells to other methods such as the hyperthermia effect. With this approach, this study introduced how adjuvant therapy with CCM strategies is optimum. In addition, spheroid models were suitable for in vitro systems simulating three-dimensional (3D) tumors. It can be used as a predictor and evaluator of responses, especially in terms of reviewing metabolite inhibitors (29). Spheroids were used in this study, and 100- 300 μ m was obtained from 10-20 days after seeding, which is consistent with previous studies. The spheroid was morphologically confirmed (figures 1a and 1b). Time was 59 h according to results of the growth curve of spheroids' VDT for treatment (figure 2). Then, the concentration of 25.09 μ M was obtained as the IC50 of CCM after a doubling time of 59 h (figure 3). To evaluate hyperthermia, CCM is washed after 24 hours, and curcumin was removed from the cell culture medium; thus, a low cell death rate and cell viability was achieved (63%). Based on similar studies, drug toxicity increases with time (34). Therefore, to evaluate the impact of CCM before and

after radiation and combine it with hyperthermia, we used MTT assay and RT-PCR.

This study reported that CCM increased the cellular sensitivity and cell death. Apoptosis can be improved with the presence of CCM in the cell environment. Moreover, CCM and hyperthermia are examples of neo-adjuvant methods that damage living tissue and cells. The use of these non-invasive and non-ionizing methods requires an optimal treatment regime based on molecular changes (26, 27, 35, 36). Thus, cell death was measured for all groups in single and combination treatments. Based on figure 4, when treatments were used alone, all the groups significantly differed from the control group (P value < 0.05). On the other hand, when the two methods were combined (IR+CCM, CCM+IR, IR+H, and CCM+H), all the groups significantly differed two by two. At the same time, the interesting point was about cell viability for the CCM+IR (60.62 ± 0.05) group compared to the CCM (after) with radiation (IR+ CCM) group (51.04 ± 0.01); the cell viability for IR+CCM group was about 9% more than the CCM (before) with radiation (CCM+IR) group (P value > 0.05). Most cell deaths were noticed in the combination group (IR+CCM+H), representing the lowest viability at 31%. Zoi (2021) (37) similarly studied the synergistic effect of CCM and radiation (2 and 4 Gy) in glioblastoma cells; the results showed that CCM sensitizes spheroids to radiation and increases cell death. It may be assumed that CCM significantly reduces the expression of DNA repair enzymes, which is often associated with chemical resistance and repair of DNA. Recently, the combination of CCM and radiation has been a controversial issue. A study showed that CCM enhances DNA damages of mytomicin (MCC) after MCC treatment in glioma. On the other hand, CCM drugs attenuate radiation and reduce the apoptosis effects of radiation in GBM (38, 39). The synergistic effect of CCM and low-dose radiation increased tumor cell death. Studies indicate that cell groups treated with CCM show G2/M arrest and the expression of p53 which indicates more apoptotic cells (34, 40).

The mechanism of anti-cancer hyperthermia is mostly due to direct cellular toxicity. Hyperthermia can eliminate hypoxic-resistant and S phase cells. It also prevents the repair of DNA of sub-lethal damages by low-dose radiation (41). Hyperthermia treatment methods based on increasing the temperature to 43 $^{\circ}$ C and above prevent DNA repair (32, 42). This effect is examined by caspase-3, Bax, and Bcl-2 as essential factors. Caspase3 is an important component of apoptotic signal transduction pathways and has been a point for these pathways' convergence. Apoptotic signaling pathways are activated after the activation of caspase-3. Bax can support cell apoptosis by inserting small molecules into the cytoplasm. Since Bcl-2 is known as an

anti-apoptosis protein, Bax also competes with Bcl-2 for apoptotic function⁽³⁶⁾.

RT-PCR was performed to measure apoptotic genes⁽²¹⁾. Upregulation of the Bax gene in all the treated groups was significantly more than in the control group (P value <0.05) (figure 5a). However, the expression of Bax and caspase-3 genes in the combination treatment, especially in IR+CCM+H (3.80 ± 0.02 and 5.13 ± 0.01 respectively), was evident. Note that the Bax and caspase-3 rate in the CCM (after) with radiation (IR+CCM) group (2.42 ± 0.02 and 3.30 ± 0.02 , respectively) was higher compared with the CCM (before) with radiation (CCM+IR) group (2.12 ± 0.02 and 2.91 ± 0.03 , respectively). In addition, there was a total increase in caspase-3, with the most expression for the IR+CCM+H (5.13 ± 0.01) group (figure 6). Nevertheless, a total decrease in the Bcl-2 rate was observed in the combination of radiation, CCM, and hyperthermia group (IR+CCM+H) (0.41 ± 0.01) (figure 5b).

Every treatment has cell death mechanisms of its own. According to the results, using the three methods intensifies this mechanism due to exacerbating cancer cell death. Besides reducing the expression of Bcl 2, CCM was also associated with increases in apoptosis and caspase3 and Bax levels in GBM cells (Figs. 5 and 6). The findings indicated that CCM can induce an intrinsic apoptotic signal and promote apoptosis in GBM cells. Dhandapni (2007)⁽³⁵⁾ reported that malignant gliomas are often resistant to radiotherapy and chemotherapy. Chemoresistance and radioresistance of gliomas increased due to the high expression levels of NF- κ B and AP-1. The finding showed that by reducing the survival of cells, CCM managed to sensitize human and rat glioma cells. CCM indicated a decrease in cell survival from the specific pathways of AP-1 and NF- κ B signaling in the treatment of T98G, U87mg, and T67 cells. Similar effects were demonstrated in a study where CCM prevented NF- κ B-mediated radioprotection and modulated human neuroblastoma cell expression of apoptosis and anti-apoptotic genes. CCM can suppress NF- κ B activity and adjust the expression of gene products of NF- κ B (cyclin D1, c-myc, Bcl-2, and Bcl-xL). Dahandapni also investigated a combination of radiation 2Gy and 100-nM CCM during 1 h in SK-N-MC human neuroblastoma cell line U87MG monolayer cells. Cell death showed that CCM sensitizes cells to radiation-induced cell death 48 h after treatment. Other studies report the effect of CCM on blocking the cell phase at the G2/M by reducing the level of expression of CDC25 and CDC2 and increasing the expression of P21. CCM also enables the inhibition of signaling phosphorylation of Akt/mTOR, reducing protein expression of Bcl-2, and increasing Bax expression caused by caspase-3 protein in the cell; eventually, cell apoptosis occurs

(40). Chendil (2004)⁽⁴³⁾ also showed that in combination with radiation, CCM at 2 and 4 μ M concentrations significantly enhanced radiation-induced clonogenic inhibition and apoptosis. CCM also has an inhibitory effect on TNF- α -mediated NF κ B activity with radiation, which reduces Bcl-2. The level of Bax protein in PC3 (human prostate cancer cell line) remained constant after radiation therapy or CCM plus the treatment of radiation therapy. In this study, the results showed a decrease in Bcl-2 and increase in Bax, which do not confirm Bax remaining constant.

Apoptosis prevention correlates with cancer development, drug resistance, and radiation resistance in glioblastoma. Karunagaran (2005)⁽⁹⁾ demonstrated that CCM promoted tumor cell apoptosis. Lohr (2000)⁽⁴⁴⁾ and Stankiewicz (2009)⁽⁴⁵⁾ also showed that hyperthermia could induce cell apoptosis via different pathways in vivo and in vitro. Tang (2013)⁽⁴⁶⁾ found a synergistic anti-tumor effect by combination therapy. Hyperthermia is a cancer treatment method that administers heat in various ways to treat malignancies. While hyperthermia alone is often not enough to eradicate the established tumors, it increases the effectiveness of drugs and radiation to cell death⁽⁴⁷⁾. Radiation-induced cell damage can be classified into several categories of DNA sub-lethal injury, potentially lethal injury, and lethal damage. In fact, DNA double-strand breakage is required to cause lethal damage⁽²⁷⁾. Studies have indicated that heating can change the distribution of the DNA double-strand break-repair protein MRE11 (the main target protein of radio-sensitization) and cellular death with the micronuclei. Moreover, denaturation of cell proteins can lead to heating, including some enzymes of DNA-repair. Repair of single and double strands is prevented due to a decrease in DNA enzyme activity, resulting in irreversible damage. In addition, heat shocks affect the kinetics of some DNA repair pathways that are instrumental in repairing damage after irradiation⁽²⁷⁾.

Cell sensitivity is much higher to radiation in the G2/M phase to temperature and hyperthermia methods and in the S phase⁽³⁵⁾. Evidence also suggests the effect of CCM on blocking the G2/M cell phase⁽⁴⁰⁾. It could be concluded that the combination of hyperthermia and radiation therapy will increase cells throughout the cell cycle. The overall result of this combined therapy can also affect the entire cellular cycle and G1 and S phase. Neshasteh-riz (2014)⁽²⁶⁾ evaluated a combination of hyperthermia and radiation on glioma spheroids by comet assay and reported the synergetic effect of these two modalities. Results indicated that this combinational therapy induced cell apoptosis. According to these findings, combining CCM nanoparticles with hyperthermia can inhibit the proliferation of cancer cells based on sub-G1 cell cycle arrest. There is also

evidence for a significant increase in caspase-3 expression and decreased viability in the CCM group when it is treated with hyperthermia.

To choose the best GBM cancer treatment regimen strategy, we investigated the effect of CCM before and after radiation. The results showed that CCM (after) with radiation (IR+CCM) is more effective than the other combination treatments (IR+H, CCM+H) two by two, and the apoptotic genes increased more than CCM (before) with radiation (CCM+IR). This finding is attributed to the CCM's radioprotective and synergistic effects on increasing the DNA damage of GBM cells. CCM can raise the Bax/Bcl-2 ratio. The Bax/Bcl-2 ratio in CCM (after) with radiation (IR+CCM) group was higher than in the radiation after CCM (before) with radiation (CCM+IR) group (figure 5b). The Bax/Bcl-2 ratio is an important landmark for apoptosis assay in cell death (21, 48). The results of this study confirmed an increase in the pro-apoptotic gene Bax and a decrease in the antiapoptotic gene Bcl-2. The potential inhibitory effect of CCM on GBM spheroid *in-vitro* was demonstrated by these results. CCM reduces the viability of GBM cells and promote GBM cell apoptosis. Moreover, CCM following radiotherapy enhances cellular damage and boosts the therapeutic efficacy of hyperthermia.

CONCLUSION

CCM with adjuvant therapy increased GBM cells' apoptosis and death. Therefore, CCM as a promising therapy for improving GBM management merits further evaluation. In cancer treatment, the combination of radiation before and after CCM was more effective than any other form of radiation. Using this method, cells also become sensitive to hyperthermia. The present findings provide an optimized CCM strategy with radiation therapy and hyperthermia cancer treatment methods.

ACKNOWLEDGEMENT

We acknowledge the help and support of the Iran University of Medical Sciences.

Funding: The Research Chancellor of the Iran University of Medicine funded this study.

Conflict of interest: There is no conflict of interest.

Ethical considerations: Ethical approval was obtained for this study [Ethics Committee No: IR.QUMS.REC.1394.26042, approval date: 2015-06-28].

Authors' contribution: Ali Neshastehriz and Bitā Ghanbari conceived and designed the study. Bitā Ghanbari collected the data and wrote first draft of the manuscript. Zeinab Hormozi-Moghaddam analyzed the data. Zeinab Hormozi-Moghaddam wrote and revised the main manuscript.

REFERENCES

- Peter K, Kar SK, Gothwal R, *et al.* (2021) Curcumin in combination with other adjunct therapies for brain tumor treatment: Existing knowledge and blueprint for future research. *International Journal of Molecular and Cellular Medicine*, **10**(3): 163-181.
- Sung H, Ferlay J, Siegel RL, *et al.* (2021) Global cancer statistics 2020: GLOBOCAN estimates of incidence and mortality worldwide for 36 cancers in 185 countries. *CA Cancer J Clin*, **71**: 209-49.
- Sigmond J, Honeywell R, Postma T, *et al.* (2009) Gemcitabine uptake in glioblastoma multiforme: potential as a radiosensitizer. *Annals of Oncology*, **20**(1): 182-187.
- Liu Y, Song X, Wu M, *et al.* (2020) Synergistic effects of resveratrol and temozolomide against glioblastoma cells: underlying mechanism and therapeutic implications. *Cancer Manag Res*, **12**: 8341-8354.
- Schwarz K, Dobiasch S, Nguyen L, *et al.* (2020) Modification of radiosensitivity by curcumin in human pancreatic cancer cell lines. *Sci Rep*, **10**(1): 3815.
- Huang BR, Tsai CH, Chen CC, *et al.* (2019) Curcumin promotes connexin 43 degradation and temozolomide-induced apoptosis in glioblastoma cells. *Am J Chin Med*, **47**(3): 657-674.
- Jäättelä M (2004) Multiple cell death pathways as regulators of tumour initiation and progression. *Oncogene*, **23**(16): 2746-2756.
- Blanquicett C, Gillespie GY, Nabors LB, *et al.* (2002) Induction of thymidine phosphorylase in both irradiated and shielded, contralateral human U87MG glioma xenografts: implications for a dual modality treatment using capecitabine and irradiation. *Mol Cancer Ther*, **1**(12): 1139-1145.
- Karunakaran D, Rashmi R, Kumar TR (2005) Induction of apoptosis by curcumin and its implications for cancer therapy. *Curr Cancer Drug Targets*, **5**(2):117-129.
- Koul D, Takada Y, Shen R, *et al.* (2006) PTEN enhances TNF-induced apoptosis through modulation of nuclear factor-kappaB signaling pathway in human glioma cells. *Biochem Biophys Res Commun*, **350**(2): 463-471.
- Nagane M, Levitzki A, Gazit A, *et al.* (1998) Drug resistance of human glioblastoma cells conferred by a tumor-specific mutant epidermal growth factor receptor through modulation of Bcl-XL and caspase-3-like proteases. *Proc Natl Acad Sci U S A*, **95**(10): 5724-5729.
- Biswas DK, Martin KJ, McAlister C, *et al.* (2003) Apoptosis caused by chemotherapeutic inhibition of nuclear factor-kappaB activation. *Cancer Res*, **63**(2): 290-295.
- Dalen H and Neuzil J (2003) α -Tocopheryl succinate sensitises a T lymphoma cell line to TRAIL-induced apoptosis by suppressing NF- κ B activation. *British Journal of Cancer*, **88**(1): 153-158.
- Pennarun G, Granotier C, Gauthier LR, *et al.* (2005) Apoptosis related to telomere instability and cell cycle alterations in human glioma cells treated by new highly selective G-quadruplex ligands. *Oncogene*, **24**(18): 2917-28.
- Shervington A, Cruickshanks N, Wright H, *et al.* (2006) Glioma: what is the role of c-Myc, hsp90 and telomerase? *Mol Cell Biochem*, **283**(1-2): 1-9.
- Woo JH, Kim YH, Choi YJ, *et al.* (2003) Molecular mechanisms of curcumin-induced cytotoxicity: induction of apoptosis through generation of reactive oxygen species, down-regulation of Bcl-XL and IAP, the release of cytochrome c and inhibition of Akt. *Carcinogenesis*, **24**(7): 1199-1208.
- Laha D, Pal K, Chowdhuri AR, *et al.* (2019) Fabrication of curcumin-loaded folic acid-tagged metal organic framework for triple negative breast cancer therapy in in vitro and in vivo systems. *New Journal of Chemistry*, **43**(1): 217-229.
- Karmakar S, Banik NL, Patel SJ, *et al.* (2006) Curcumin activated both receptor-mediated and mitochondria-mediated proteolytic pathways for apoptosis in human glioblastoma T98G cells. *Neurosci Lett*, **407**(1): 53-58.
- Anto RJ, Mukhopadhyay A, Denning K, *et al.* (2002) Curcumin (diferuloylmethane) induces apoptosis through activation of caspase-8, BID cleavage and cytochrome c release: its suppression by ectopic expression of Bcl-2 and Bcl-xL. *Carcinogenesis*, **23**(1): 143-150.
- Duvoix A, Blasius R, Delhalle S, *et al.* (2005) Chemopreventive and therapeutic effects of curcumin. *Cancer Lett*, **223**(2): 181-190.
- Moloudi K, Neshasteriz A, Hosseini A, *et al.* (2017) Synergistic Effects of Arsenic Trioxide and Radiation: Triggering the Intrinsic Pathway of Apoptosis. *Iran Biomed J*, **21**(5): 330-337.
- Su X, Chen S, Lu H, *et al.* (2021) Study on the inhibitory effect of

- curcumin on GBM and its potential mechanism. *Drug Des Devel Ther*, **15**: 2769-2781.
23. Lee Y-J, Park K-S, Lee S-H (2021) Curcumin targets both apoptosis and necroptosis in acidity-tolerant prostate carcinoma cells. *Bio-Med Research International*, **2021**: 8859181.
 24. Kim JY, Jung CW, Lee WS, et al. (2022) Interaction of curcumin with glioblastoma cells via high and low linear energy transfer radiation therapy inducing radiosensitization effects. *J Radiat Res*, **63**(3): 342-353.
 25. Hildebrandt B, Wust P, Ahlers O, et al. (2002) The cellular and molecular basis of hyperthermia. *Crit Rev Oncol Hematol*, **43**(1): 33-56.
 26. Neshasteh-Riz A, Rahdani R, Mostaar A (2014) Evaluation of The Combined Effects of Hyperthermia, Cobalt-60 Gamma Rays and IUDR on cultured glioblastoma spheroid cells and dosimetry using TLD-100. *Cell J*, **16**(3): 335-342.
 27. Rao W, Deng ZS, Liu J (2010) A review of hyperthermia combined with radiotherapy/chemotherapy on malignant tumors. *Crit Rev Biomed Eng*, **38**(1): 101-116.
 28. Feist M, Huang X, Müller JM, et al. (2014) Can hyperthermic intraperitoneal chemotherapy efficiency be improved by blocking the DNA repair factor COP9 signalosome? *Int J Colorectal Dis*, **29**(6): 673-680.
 29. Khaite D, Chandna S, Arya MB (2006) Establishment and characterization of multicellular spheroids from a human glioma cell line; Implications for tumor therapy. *Journal of Translational Medicine*, **4**(1): 12.
 30. Carlsson J and Yuhas JM (1984) Liquid-overlay culture of cellular spheroids. *Recent Results Cancer Res*, **95**: 1-23.
 31. McFadden RM, Larmonier CB, Shehab KW, et al. (2015) The role of curcumin in modulating colonic microbiota during colitis and colon cancer prevention. *Inflamm Bowel Dis*, **21**(11): 2483-2494.
 32. Mittal L, Aryal UK, Camarillo IG, et al. (2020) Effective electrochemotherapy with curcumin in MDA-MB-231-human, triple negative breast cancer cells: A global proteomics study. *Bioelectrochemistry*, **131**: 107350.
 33. Zhu JY, Yang X, Chen Y, et al. (2017) Curcumin suppresses lung cancer stem cells via inhibiting wnt/ β -catenin and sonic hedgehog pathways. *Phytother Res*, **31**(4): 680-688.
 34. Qian Y, Ma J, Guo X, et al. (2015) Curcumin enhances the radiosensitivity of U87 cells by inducing DUSP-2 up-regulation. *Cell Physiol Biochem*, **35**(4): 1381-1393.
 35. Dhandapani KM, Mahesh VB, Brann DW (2007) Curcumin suppresses growth and chemoresistance of human glioblastoma cells via AP-1 and NF κ B transcription factors. *J Neurochem*, **102**(2): 522-538.
 36. Elmore S (2007) Apoptosis: a review of programmed cell death. *Toxicol Pathol*, **35**(4): 495-516.
 37. Zoi V, Galani V, Vartholomatos E, et al. (2021) Curcumin and radiotherapy exert synergistic anti-glioma effect *in-vitro*. *Biomedicines*, **9**(11).
 38. Aravindan N, Veeraraghavan J, Madhusoodhanan R, et al. (2011) Curcumin regulates low-linear energy transfer γ -radiation-induced NF κ B-dependent telomerase activity in human neuroblastoma cells. *Int J Radiat Oncol Biol Phys*, **79**(4): 1206-1215.
 39. Faqih F, Neshastehriz A, Soleymannifard S, et al. (2015) Radiation-induced bystander effect in non-irradiated glioblastoma spheroid cells. *J Radiat Res*, **56**(5): 777-783.
 40. Hu S, Xu Y, Meng L, et al. (2018) Curcumin inhibits proliferation and promotes apoptosis of breast cancer cells. *Exp Ther Med*, **16**(2): 1266-1272.
 41. Iliakis G, Wu W, Wang M (2008) DNA double strand break repair inhibition as a cause of heat radiosensitization: re-evaluation considering backup pathways of NHEJ. *Int J Hyperthermia*, **24**(1): 17-29.
 42. Takahashi A, Matsumoto H, Nagayama K, et al. (2004) Evidence for the involvement of double-strand breaks in heat-induced cell killing. *Cancer Res*, **64**(24): 8839-8845.
 43. Chendil D, Ranga RS, Meigooni D, et al. (2004) Curcumin confers radiosensitizing effect in prostate cancer cell line PC-3. *Oncogene*, **23**(8): 1599-1607.
 44. Lohr F, Hu K, Huang Q, et al. (2000) Enhancement of radiotherapy by hyperthermia-regulated gene therapy. *Int J Radiat Oncol Biol Phys*, **48**(5): 1513-1518.
 45. Stankiewicz AR, Livingstone AM, Mohseni N, et al. (2009) Regulation of heat-induced apoptosis by Mcl-1 degradation and its inhibition by Hsp70. *Cell Death Differ*, **16**(4): 638-647.
 46. Tang JC, Shi HS, Wan LQ, et al. (2013) Enhanced antitumor effect of curcumin liposomes with local hyperthermia in the LL/2 model. *Asian Pac J Cancer Prev*, **14**(4): 2307-2310.
 47. Helleday T, Petermann E, Lundin C, et al. (2008) DNA repair pathways as targets for cancer therapy. *Nat Rev Cancer*, **8**(3): 193-204.
 48. Wust P, Hildebrandt B, Sreenivasa G, et al. (2002) Hyperthermia in combined treatment of cancer. *Lancet Oncol*, **3**(8): 487-497.

